Quantitative Interpretations of Break Junction Conductance Histograms in Molecular Electron Transport

Robert Quan,[†] Christopher S. Pitler,[†] Mark A. Ratner,[‡] and Matthew G. Reuter*[,‡,§]

[†]Department of Materials Science and Engineering and [‡]Department of Chemistry, Northwestern University, Evanston, Illinois 60208, United States and [§]Department of Applied Mathematics & Statistics and Institute for Advanced Computational Science, Stony Brook University, Stony Brook, New York 11794, United States

ABSTRACT We develop theoretical and computational tools for extracting quantitative molecular information from experimental conductance histograms for electron transport through single-molecule break junctions. These experimental setups always measure a combination of molecular conductance and direct electrode–electrode tunneling; our derivations explicitly incorporate the effects of such background tunneling. Validation of our models to simulated data shows that background tunneling is crucial for quantitative analyses (even in cases where it appears to be qualitatively negligible), and comparison to experimental data is favorable. Finally, we generalize these ideas to the case of molecules with a destructive interference feature and discuss potential signatures for interference in a conductance histogram.

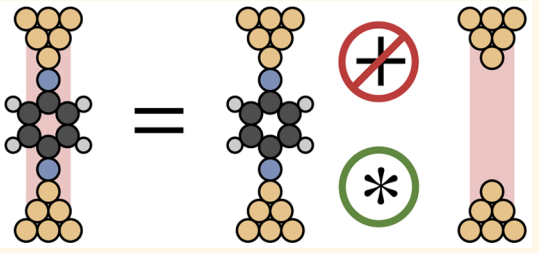

KEYWORDS: molecular electronics · conductance histograms · break junctions · tunneling

The determination of a single molecule's electronic properties when connected between two electrodes has become an active research area in recent years.[1−4] Some of this interest is due to fundamental curiosity into how molecules, which are inherently quantum mechanical, transport electrons. Other interest, however, is more applied and seeks to incorporate molecules into electronic devices,[5] including sensors, photovoltaics, or thermoelectrics. Regardless of the motivation, these studies have found that understanding the flow of electric current through molecules is both theoretically and experimentally challenging.

The main theoretical difficulty is accounting for the massive system size when the molecule couples to two electrodes to form a junction. Essentially, the molecular levels become conduction channels[6] through the junction, which are scattering states with well-defined probabilities of transmitting an electron between the electrodes. Then, in the limit of elastic scattering, the Landauer–Büttiker theory[3,7,8] describes the steady-state electronic properties of the junction. For instance, the zero-bias conductance, G, is given by

$$G = G_0 \sum_j T_j(E_F) \qquad (1)$$

where $G_0 \equiv 2e^2/h$ is the quantum of conductance, E_F is the junction's Fermi energy, and $T_j(E)$ is the probability that channel j transmits an electron with energy E from one electrode to the other. In this sense, conductance is transmission.[8]

Experimentally, the primary challenges are fabricating and characterizing single-molecule junctions.[9,10] Break junction techniques,[9−17] which will be discussed more later, meet this need and have become common in experimental studies. Although effective at characterizing the conductance through a molecular junction, these techniques are generally unable to determine *or control* the microscopic geometry of the junction (such as binding geometry and electrode shape).[18−21] Molecular conductance is extremely sensitive to these details;[22−25] thus, there is considerable variation from one experimental measurement to another. The "molecular conductance"

* Address correspondence to matthew.reuter@stonybrook.edu.

Received for review May 26, 2015 and accepted July 13, 2015.

Published online July 13, 2015
10.1021/acsnano.5b03183

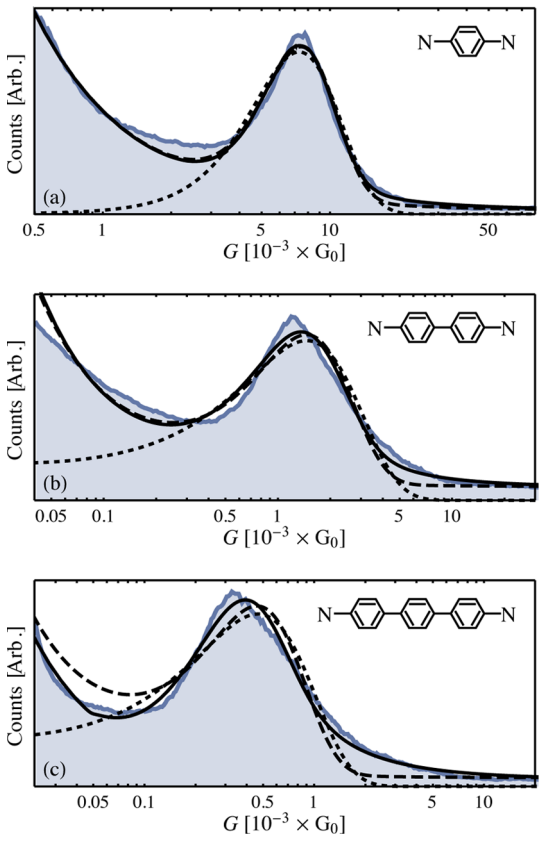

Figure 1. Conductance histograms for (a) 1,4-diaminobenzene, (b) 4,4′-diaminobiphenyl, and (c) 4,4″-diaminoterphenyl connected between gold electrodes. The insets show the molecular structures with protons omitted for simplicity. A molecular peak (approximately centered) is present along with a "signal" for only background tunneling to the left. In all panels, the blue line is experimental data, the dotted black line is the fit for only molecular tunneling (eq 3), the dashed black line is the fit for independent tunneling through the molecule and the background (eq 7), and the solid black line is the fit for combined tunneling through the molecule and the background (eq 9). The fit parameters are displayed in Table 2. In all three examples, neglecting background tunneling underestimates the level alignment between the molecular channel and the junction Fermi energy (*i.e.*, c_ε is underestimated). These experimental data are used, with permission, from ref 20.

can only be statistically interpreted from many measurements,[19] often thousands or more.

To aid in this analysis, measurements are compiled into a conductance histogram, which reports the relative probability that a particular conductance was observed.[9,10,13,14,20,26,27] Example experimental conductance histograms are shown in Figure 1. These histograms each exhibit a peak that is attributed to conductance through the molecule.[10,13,20] The mode of the peak is taken to be the molecular conductance, and its width is a convolution of many chemical factors,[28−32] including temperature and solvent.

Despite the irreproducibility of each experimental measurement, the histogram *is* reproducible (assuming a sufficient number of measurements). More recent studies have consequently investigated the information content of a conductance histogram peak[33−37] and developed theories for extracting deeper physical insights from experimental data. For example, a single-channel molecular histogram peak encodes quantitative information on (i) the channel's level alignment and (ii) the molecule−electrode coupling strength(s).[34,36]

Most analyses, however, ignore the presence of direct electrode−electrode tunneling, which leads to the monotonically decaying "signal" at the left of the histograms.[33,38−40] Such background tunneling is always measured—in addition to molecular tunneling—and can qualitatively change the molecular histogram peak.[33] Experimental and theoretical efforts to disentangle molecular conductance from the background have been developed; however, they often require processing the individual measurements before compiling a histogram. Data selection might be used on the experimental side,[15,18,29,39,41−44] where measurements without a clear molecular signal are discarded. Theoretical studies have regarded the direct electrode−electrode tunneling as an extra channel through the junction[33,39] and subsequently proposed methods to extract only the molecular conductance from each measurement.[33] We discuss these ideas in more detail below.

In this work, we go beyond these approaches and consider the quantitative ramifications of background tunneling directly on a conductance histogram. By combining probability theory[45] with the Landauer−Büttiker theory for molecular electron transport, we first derive functional forms (*e.g.*, eq 9) for fitting conductance histograms that include background tunneling *and* have physically significant fitting parameters.[36] We then demonstrate the utility of these models on simulated and experimental conductance histograms, showing that they *faithfully* quantify properties of the molecule. Ultimately, our results show that background tunneling significantly impacts quantification of the molecular properties underlying electron transport. It must be taken into account.

The layout of this paper is as follows. We first elaborate on conductance histograms, providing an overview of break junction techniques and of existing theory for analyzing a histogram. Then we develop, validate, and apply tools to account for background tunneling in the line shape of a histogram peak. We also offer, at the end of the Results and Discussion section, our thoughts on how background tunneling relates to the observation of destructive interference features[46−55] in single-molecule electron transport.

RESULTS AND DISCUSSION

Break Junctions and Conductance Histograms. Break junction techniques[16,17] are common for measuring the electron transport properties of single molecules

bridging two electrodes.[9−15,26] Each break junction experiment produces a conductance trace, which reports the conductance as a function of the distance between the two electrodes. As it suffices for our purposes, a molecule can diffuse into the junction when the electrodes are adequately separated. Conductance through the resulting molecular junction is measured and appears as a plateau in the conductance trace; that is, the conductance is relatively stable with respect to changes in the electrode separation.

Break junction techniques cannot control the microscopic geometry of the junction (that is, the exact atomic geometry of the electrodes and molecule); as a result, there is substantial variability from one conductance trace to the next. In the simplest cases, the molecule couples to the electrodes differently and the molecular plateau appears around a slightly different conductance. In other cases, a molecule may not bridge the gap—no junction forms—and the entire molecular plateau is omitted. Finally, the presence (absence) of a molecular plateau is not clear in some cases.

With our focus on conductance through molecules, it might appear that only the molecular plateaux are of interest. Along these lines, various techniques for selecting the traces with plateaux have been developed,[15,18,29,39,41,42,44] where conductance traces without identifiable plateaux are excluded from further statistical analyses. This idea seems helpful for isolating the molecular conductance but has several drawbacks. First, these data selection procedures can qualitatively alter the statistics.[33,39] For example, a histogram peak may change shape or even (dis)appear depending on the data selection method. Second, although data selection eliminates traces without molecular conductance, it does not address the ubiquity of background tunneling within the molecular plateaux.

Two noteworthy ideas have been subsequently reported to tackle these issues. First, pertaining to the use of data selection schemes, ref 43 shows that background tunneling alone should result in a conductance histogram proportional to $1/G$. Consequently, a conductance histogram produced by logarithmically binning (*i.e.*, binning in $\ln G/G_0$ rather than G) *all* conductance traces should display the background as a horizontal line. Subtraction then trivially removes the background-only traces from the histogram. Second, ref 33 discusses a method to disentangle the molecular conductance from the background, assuming an identifiable plateau. In short, fitting each trace/plateau to a prescribed functional form separates the two contributions. The resulting molecular conductances are then binned into a histogram and analyzed.

In what follows, we essentially combine these two approaches to deconvolve molecular conductance from the background at the level of conductance histograms (not traces), thereby erasing the requirement for identifiable conductance plateaux. Before proceeding, though, we review existing theory for conductance histograms that only consider contributions from a single molecule.

Our theory for conductance histograms[35,36] begins by likening experimental uncertainty to stochasticity. In other words, every time conductance is measured, the junction's geometry is sampled from a distribution of possible geometries. The conductance histogram is then the probability density function[45] for the conductance observable. We now describe how to combine probability theory[45] and the Landauer−Büttiker theory for electron transport to statistically relate measured conductance values to microscopic geometric details.

First, we must determine the key physical parameters underlying single-molecule electron transport. The Landauer−Büttiker theory is useful here. In the limit that only a single molecular conduction channel contributes to transport (which is reasonable for many molecules[56]), the transmission function usually has a quasi-Lorentzian form[37]

$$T_{\text{molecule}}(E) = \frac{4\Gamma_L\Gamma_R}{4(E-\varepsilon)^2+(\Gamma_L+\Gamma_R)^2}$$

where ε is the channel's resonance energy, $\Gamma_L > 0$ is the coupling strength (dimension of energy) between the channel and the left electrode, and similarly for $\Gamma_R > 0$ with the right electrode. Moreover, the molecular channel is often far from resonance; that is, $4(E-\varepsilon)^2 \gg (\Gamma_L+\Gamma_R)^2$. Then

$$T_{\text{NR}}(E) \approx \frac{\Gamma^2}{(E-\varepsilon)^2} \tag{2}$$

where $\Gamma \equiv (\Gamma_L\Gamma_R)^{1/2}$ is an effective molecule−electrode coupling element. The "NR" subscript denotes nonresonant tunneling. For reference, Table 1 lists the symbols and meanings for these quantities and those that appear below.

Consequently, the two principal physical parameters underlying single-molecule electron transport are (i) the channel's resonance energy, ε, and (ii) the channel−electrode coupling, Γ. Turning to conductance histograms, we assume that ε and Γ are independent (for simplicity) random variables, and that each measurement samples from their respective statistical distributions. The probability density function of the conductance observable (that is, the line shape of the histogram peak) is then given by[36]

$$\mathscr{P}_{\text{NR}}(g) \propto \int_{-\infty}^{\infty} d\varepsilon \int_0^{\infty} d\Gamma \mathscr{P}_\varepsilon(\varepsilon)\mathscr{P}_\Gamma(\Gamma)\delta[g - T_{\text{NR}}(E_F)]$$

where $\mathscr{P}_\varepsilon(\varepsilon)$ is the probability density function for ε, likewise for $\mathscr{P}_\Gamma(\Gamma)$, and $g \equiv G/G_0$ (requiring conductance to be in atomic units simplifies the presentation by eliminating numerous G_0 factors). In words, the above expression counts all combinations of ε and Γ

TABLE 1. Glossary of Key Symbols (Quantities Are Dimensionless unless Otherwise Noted)

symbol	quantity
G	conductance (dimension of conductance)
g	G/G_0; conductance in atomic units
$T(E)$	probability that a channel transmits an electron with energy E
ε	channel energy (dimension of energy)
Γ	channel−electrode coupling (dimension of energy)
ω	transmission well "steepness" (dimension of energy)
$\mathscr{P}(g)$	probability density function or conductance histogram line shape
$\mathscr{P}_{\mathrm{NR}}$	histogram line shape for only nonresonant tunneling through the molecule
$\mathscr{P}_{\mathrm{background}}$	histogram line shape for only background tunneling
$\mathscr{P}_{\mathrm{NR+background}}$	histogram line shape for independent tunneling through the molecule and the background
$\mathscr{P}_{\mathrm{NR*background}}$	histogram line shape for simultaneous tunneling through the molecule and the background
$\mathscr{P}_{\mathrm{experiment}}$	histogram line shape for describing experimental data; includes $\mathscr{P}_{\mathrm{NR*background}}$ and pure background tunneling
$\mathscr{P}_{\mathrm{interference}}$	histogram line shape for transport near a destructive interference feature
$\mathscr{P}_{\mathrm{interference*background}}$	histogram line shape for simultaneous tunneling through the background and a destructive interference feature
c_ε	fitting parameter for $\mathscr{P}_{\mathrm{NR}}$ that relates to the average level alignment
c_Γ	fitting parameter for $\mathscr{P}_{\mathrm{NR}}$ that relates to the average coupling strength
g_-	fitting parameter for the threshold conductance in $\mathscr{P}_{\mathrm{background}}$
c_ω	fitting parameter for $\mathscr{P}_{\mathrm{interference}}$

that produce a junction with conductance g, weighted by the probability of finding such a junction. Note the proportionality relation instead of outright equality because experimental conductance histograms are often arbitrarily normalized.

If we further assume that both the resonance energy and the coupling strength are normally distributed (notationally, $\mathscr{P}_\varepsilon$ has average $\tilde{\varepsilon}$ and standard deviation δ_ε and similarly for $\mathscr{P}_\Gamma$), the integral evaluates to[36]

$$\mathscr{P}_{\mathrm{NR}}(g) \propto \frac{1}{\sqrt{g(1-g)^3}} \exp\left[-\frac{(c_\varepsilon\sqrt{g} - c_\Gamma\sqrt{1-g})^2}{2(1-g)}\right] \tag{3}$$

where $c_\varepsilon \equiv |E_F - \tilde{\varepsilon}|/\delta_\Gamma$ relates to the average level alignment ($|E_F - \tilde{\varepsilon}|$) and $c_\Gamma \equiv \tilde{\Gamma}/\delta_\Gamma$ relates to the average coupling strength. Equation 3 thus provides a functional form—with physically significant parameters—for fitting a single-molecule conductance histogram peak. Examples of fits to eq 3 are shown as dotted lines in Figure 1. As a side note, recent experimental studies have further validated this form[57] and also investigated the distributions of ε and Γ.[57,58]

Finally, ref 35 uses probability theory to consider the line shape of a histogram peak corresponding to transport through two channels, given the line shape through each channel independently. To summarize, the probability density function for conductance through both channels is

$$\mathscr{P}_{1+2}(g) \propto \int_0^1 dg_1 \int_0^1 dg_2 \mathscr{P}_1(g_1)\mathscr{P}_2(g_2)\delta(g - g_1 - g_2)$$

where the "1" and "2" subscripts denote the channels. This formula assumes that the two channels are statistically uncorrelated; that is, knowing the conductance through channel 1 (g_1) tells us nothing about the conductance through channel 2 (g_2). Then, by integrating out the δ function

$$\mathscr{P}_{1+2}(g) \propto \int_{\max(0,\, g-1)}^{\min(g,\, 1)} dg' \mathscr{P}_1(g')\mathscr{P}_2(g - g') \tag{4}$$

The line shape of a conductance histogram peak for two channels is the convolution of the line shape for each channel independently.

Background Tunneling Only. We now derive a histogram line shape for background tunneling only. To start, we use a rectangular barrier model[59] to describe the direct electrode−electrode tunneling, where an electron tunnels through a barrier of energy height V and spatial width w. As discussed in the Supporting Information, the transmission probability is given by

$$T_{\mathrm{background}}(E) \approx \frac{16E}{V} \exp\left[-2\frac{\sqrt{2mV}}{\hbar}w\right] \tag{5}$$

If we assume that each junction has a slightly different barrier (the width and/or height fluctuate), the histogram line shape is

$$\mathscr{P}_{\mathrm{background}}(g) \propto \int_0^\infty dV \int_0^\infty dw \mathscr{P}_V(V)\mathscr{P}_w(w)\delta[g - T_{\mathrm{background}}(E_F)]$$

To mimic experiments, where the electrode separation is commonly increased at a constant speed, we take w to be uniformly distributed between two distances. A log-normal distribution is used for V because it provides analytical results. (We do not expect the results to substantially change if a different unimodal distribution is used instead.) For brevity, evaluation of this integral is relegated to the Supporting Information and leads to

$$\mathscr{P}_{\mathrm{background}}(g) \propto \frac{\Theta(g - g_-)}{g} \tag{6}$$

TABLE 2. Model Parameters for the Fits of Experimental Data in Figure 1[a]

Figure	model	c_ε	c_Γ	g_-
1a	$\mathscr{P}_{NR}$	53	4.7	
	$\mathscr{P}_{NR+background}$	63	5.7	
	$\mathscr{P}_{experiment}$	67	5.9	5.0×10^{-9}
1b	$\mathscr{P}_{NR}$	69	3.0	
	$\mathscr{P}_{NR+background}$	84	3.5	
	$\mathscr{P}_{experiment}$	92	3.4	9.0×10^{-6}
1c	$\mathscr{P}_{NR}$	120	2.9	
	$\mathscr{P}_{NR+background}$	140	3.4	
	$\mathscr{P}_{experiment}$	170	2.7	4.9×10^{-5}

[a] The functional forms for $\mathscr{P}_{NR}$ (molecule only), $\mathscr{P}_{NR+background}$ (molecule and background independently), and $\mathscr{P}_{experiment}$ (convolved molecule and background) are found in eqs 3, 7, and 9, respectively.

where Θ is the Heaviside step function and g_- is a threshold conductance that depends on the $\mathscr{P}_w$ and $\mathscr{P}_V$ distributions.

Equation 6 is very similar to the $1/G$ form reported in ref 43; the only difference is the threshold conductance. In essence, we should only observe $g = 0$ when the electrodes are infinitely far apart. Because experiments always stop at some finite separation, the conductance never drops to 0 and the histogram should exhibit a threshold. As mentioned in the Supporting Information, g_- is not rigorously a constant; it depends on the tunneling barrier's fluctuations. However, we expect the range of thresholds to be small and opt, for simplicity, to take g_- itself as the fitting parameter.

Molecular and Background Tunneling. Equation 3 or 6 describes the line shape of a conductance histogram when conductance from only the molecule (*via* nonresonant tunneling) or only the background is present, respectively. We now discuss combining the two components to better understand experimental conductance histograms. The key premise mirrors ref 33: direct electrode−electrode tunneling is an additional channel through the junction.

As a baseline, Figure 1 shows fits of experimental data to the molecule-only model ($\mathscr{P}_{NR}$, dotted lines) and Table 2 lists the best-fit c_ε and c_Γ parameters. Because this model only considers conductance from the molecule, the fits fail to capture the background signal at low g and also decay too rapidly at higher g. The molecular model may be reasonable for the 1,4-diaminobenzene peak (Figure 1a); however, the fit quality deteriorates for the other two examples. For example, the fits slightly exaggerate the locations of the peaks.

Let us now incorporate the background and attempt to improve upon these deficiencies. For a first effort, we follow ref 43: subtract the background and fit what remains to the molecular line shape. In essence, we fit to

$$\mathscr{P}_{NR+background}(g) \propto \mathscr{P}_{NR}(g) + \frac{N_{background}}{g} + N_{baseline} \quad (7)$$

where the molecular and background components are trivially added together. $N_{background}$ is a scaling constant (to balance the two components), and $N_{baseline}$ is a baseline seen in experimental histograms. Figure 1 displays fits to this model as dashed lines; the corresponding c_ε and c_Γ parameters are listed in Table 2.

Qualitatively, this molecule and background model does not drastically change the fit near the molecular peak. For obvious reasons, the fit improves around the background signal (although it is still far from ideal in Figure 1c), and it transitions between the background and molecular peak a little better. Because the background rapidly decays as g increases, eq 7 does not substantially change the tails to the right of the peaks. Including the baseline actually has a greater effect here than the background.

Quantitatively, and as expected from ref 33, the level alignment (c_ε) is significantly underestimated when background tunneling is neglected. Because background tunneling has the nonuniform, $1/g$ line shape in the histogram, the observed peak is at larger conductances than a corresponding peak with only the molecular contribution. Larger conductance is generally related to a closer level alignment; thus, c_ε from the molecule-only fit should be too small. Despite only minor changes in the looks of the fits, background tunneling changes the estimates of c_ε and c_Γ by ~20%. Background tunneling is crucial when quantitatively analyzing conductance histograms.

Although the above model eliminates the perceived need for data selection—the $1/g$ term handles cases that fail to form a molecular junction—it does not account for the ubiquitous presence of background tunneling when measuring molecular conductance. Following previous work,[33] we can regard the background as an additional "channel" through the molecular junction and use eq 4 to predict the line shape for simultaneous molecular and background tunneling. Accordingly,

$$\mathscr{P}_{NR*background}(g) \propto \int_0^g dg' \mathscr{P}_{NR}(g - g')\mathscr{P}_{background}(g') \propto \int_{g_-}^g dg' \frac{\mathscr{P}_{NR}(g - g')}{g'} \quad (8)$$

for $g \geq g_-$. This line shape has three fitting parameters from the underlying models: c_ε, related to the molecular level alignment; c_Γ, related to the molecule−electrode coupling strength; and g_-, the background tunneling threshold conductance. Note that, in this context, g_- is the minimum background conductance measured with the molecular conductance, not the overall minimum background conductance.

Let us now examine several properties of eq 8 before applying it to experimental data. First, $\mathscr{P}_{NR*background}(g) = 0$ for $g < g_-$ because g_- is the minimum amount of background tunneling. Second,

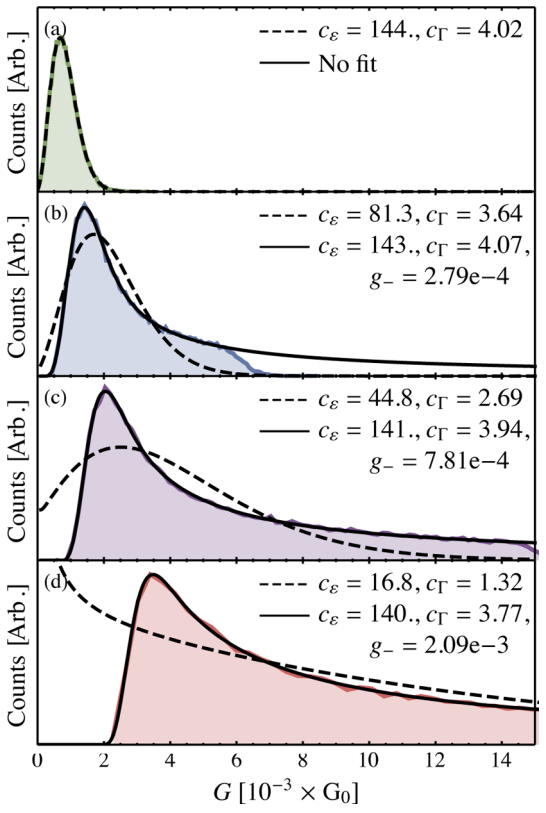

Figure 2. Simulated conductance histograms for nonresonant transport through a model molecular junction with c_ε = 143 and c_Γ = 4.00. (a) Tunneling through the bare molecule. (b–d) Tunneling through the same molecule with "small", "medium", and "large" amounts of background tunneling, respectively. In all panels, the colored line is the simulated conductance histogram, the dashed black line is the fit for tunneling through the molecule only (eq 3), and the solid black line is the fit for combined tunneling through the molecule and the background (eq 8). The fit parameters are displayed in each panel. As the amount of background tunneling increases (relative to the molecular tunneling), the estimates of c_ε and c_Γ from the molecule-only model deteriorate, whereas the combined molecule and background model consistently provides favorable agreement. Note that the molecule and background model did not produce a good fit for the histogram in panel (a) because of numerical issues arising from the absence of background tunneling.

the differences between $\mathscr{P}_{\text{NR*background}}$ and $\mathscr{P}_{\text{NR}}$ increase as g_- becomes larger; that is, background tunneling distorts the line shape. This effect is demonstrated in Figure 2. The dashed black line in Figure 2a shows the line shape for only molecular conductance with c_ε = 144 and c_Γ = 4.02. The solid black lines in Figure 2b–d then show line shapes for incrementally increased values of g_- and similar c_ε and c_Γ (*vide infra*). As the threshold increases, the peak not only moves to higher conductances[33] but also develops a longer tail to higher conductance values. Background tunneling is both quantitatively and qualitatively important.

Third, because eq 8 is nonlinear in its fitting parameters, we must verify that fitting to eq 8 *faithfully* estimates the molecular quantities c_ε and c_Γ; that is, we confirm that values of c_ε and c_Γ obtained from fitting match the actual values. To this end, the general procedure from ref 37 is used to simulate histograms with known values of c_ε and c_Γ and varying amounts of background tunneling. The resulting histograms are then fit to eq 8 so that values of c_ε and c_Γ can be compared against the "true" values.

Along these lines, Figure 2 also shows a representative set of simulated histograms and fits to both the molecule-only ($\mathscr{P}_{\text{NR}}$) and combined molecule and background ($\mathscr{P}_{\text{NR*background}}$) models. In the absence of background tunneling, Figure 2a, the combined molecule and background model encounters numerical difficulties: the integrand becomes singular as $g_- \to 0$. However, as expected,[36] the molecule-only model successfully estimates c_ε and c_Γ in this case. For a "small" amount of background tunneling (relative to the molecular conductance), Figure 2b, the molecule-only model poorly estimates c_ε (~40% relative error) and c_Γ (~10% error). When the background is taken into account, the fit looks better at a quick glance and also provides remarkably good estimates of c_ε and c_Γ (within 2%). The quality of fit from the molecule-only model degrades as background tunneling increases (Figure 2c) until the model misses the peak altogether and focuses on the tail (Figure 2d). In both of these cases, the molecule and background model faithfully estimates c_ε and c_Γ (~2–3% error).

Finally, having demonstrated the reliability of fitting conductance histograms with $\mathscr{P}_{\text{NR*background}}$, we apply the model to the experimental histograms in Figure 1. Because these histograms also contain conductance traces that lack molecular plateaux, the background-only and baseline components of eq 7 are added back in. The functional form for fitting is

$$\mathscr{P}_{\text{experiment}}(g) \propto \mathscr{P}_{\text{NR*background}}(g) + \frac{N_{\text{background}}}{g} + N_{\text{baseline}} \tag{9}$$

The solid lines in Figure 1 show the fits to this model. Qualitatively, this model captures each peak's tail to higher conductances and also provides somewhat better descriptions of each peak at lower conductances. Quantitatively, Table 2 shows that the estimates of c_ε are changed by another ~10% over the $\mathscr{P}_{\text{NR}+\text{background}}$ model. Estimates of c_Γ also change, however, in a less uniform way. Overall, eq 9 provides a reliable functional form for quantitatively interpreting conductance histograms from break junction experiments. It is not enough to simply subtract the background, the molecular conductance must further be disentangled from the background.

Tunneling near a Destructive Interference Feature. The previous subsection demonstrated the importance of background tunneling in molecular conductance histograms. The underlying assumption was that electron transport occurred *via* nonresonant tunneling; that is, the transmission function looked like eq 2 near the

Fermi energy. Although this condition is satisfied in many cases, there are counter examples, preeminently, molecules with destructive interference features.[46−55]

Destructive interference features can arise when there are multiple pathways through the molecule. As a consequence of quantum mechanics, superposition of all possible pathways may lead to destructive interference, where the transmission (through one channel) drops to 0. This effect has no known analog in conventional electronics and, consequently, has been a subject of intense interest. Despite being theoretically predicted some time ago,[46−50] these interference features were only recently experimentally observed.[60−67] The main limitation was that, because the candidate molecules have very low conductances, any peaks or features in the conductance histogram essentially get overshadowed by the background.

In the rest of this section, we apply the tools developed above for handling background tunneling to the case of destructive interference features. Ultimately, we make predictions about the signatures of interference features in conductance histograms: despite the absence of a clear peak, the shape of the conductance histogram may still provide evidence for interference.

First, we need to understand the line shape of a conductance histogram if only the molecule (with a destructive interference feature) was present. The simplest system that displays interference is a two-site tight-binding model where both electrodes couple to the same site;[50] it is similar to a stub resonator. Building on notation from above, let ε be the energy of the two degenerate "atomic" sites, Γ be the coupling element between the one site and either electrode, and β be the intersite coupling. The transmission function is (see the Supporting Information)

$$T(E) = \frac{\Gamma^2(E-\varepsilon)^2}{[(E-\varepsilon)^2-\beta^2]^2+(E-\varepsilon)^2\Gamma^2}$$

If we focus on $E \approx \varepsilon$ in the denominator, the transmission can be approximated by the parabola

$$T_{\text{interference}}(E \approx \varepsilon) \approx \frac{(E-\varepsilon)^2}{\omega^2} \qquad (10)$$

where $\omega \equiv \beta^2/\Gamma$ is essentially the steepness of the well. The two important physical parameters are now ε and ω.

Let us further suppose that ε and ω are independent random variables, such that (for E_F near the interference)

$$\mathscr{P}_{\text{interference}}(g) \propto \int_{-\infty}^{\infty} d\varepsilon \int_{0}^{\infty} d\omega \mathscr{P}_{\varepsilon}(\varepsilon)\mathscr{P}_{\omega}(\omega) \times \delta[g - T_{\text{interference}}(E_F)]$$

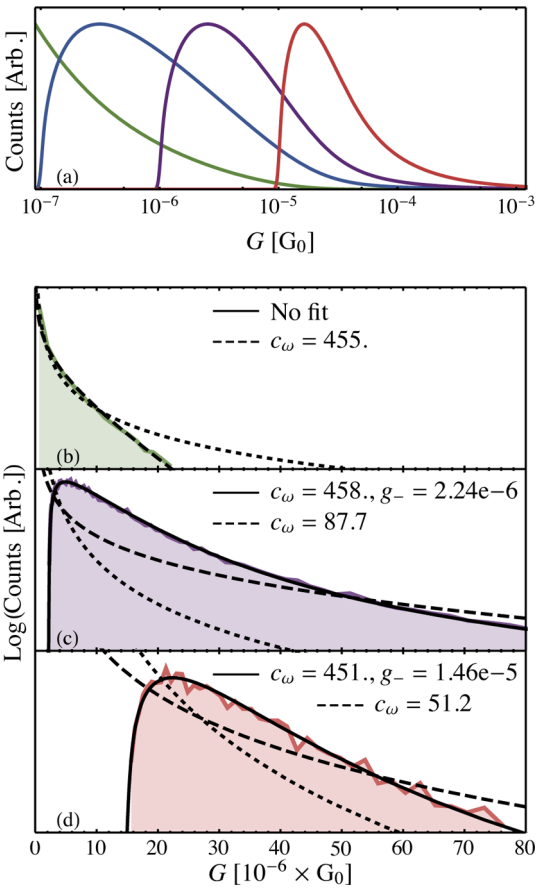

Figure 3. (a) Conductance histogram line shapes for tunneling near a destructive interference. Green line: interference only (no background tunneling). Blue, purple, and red lines: increasing amounts of background tunneling combined with the same interference feature. (b−d) Simulated conductance histograms for transport near a destructive interference with c_ω = 450, combined with (b) no background tunneling, (c) a "small" amount of background tunneling, and (d) a "large" amount of background tunneling. In all panels, the colored line is the simulated conductance histogram, the dotted black line is the fit for background tunneling only [1/g], the dashed black line is the fit for tunneling around the interference only (eq 11), and the solid black line is the fit for combined tunneling through the interference and the background (eq 12). The fit parameters are displayed in each panel. Note the log scale on the y-axes to highlight the tails of the various models as G becomes large. As the amount of background tunneling increases, the estimate of c_ω from the interference-only model deteriorates, whereas the interference and background model consistently provides favorable agreement. Similar to Figure 2, the interference and background model did not produce a good fit for the histogram in panel (b) because of numerical issues arising from the absence of background tunneling.

If ε and ω are both normally distributed (for simplicity), the integral evaluates to (see the Supporting Information)

$$\mathscr{P}_{\text{interference}}(g) \propto \frac{1}{\sqrt{g}} \exp\left[-\frac{c_\omega^2 g}{2}\right] \qquad (11)$$

where $c_\omega \equiv \tilde{\omega}/\delta_\varepsilon$ is the only fitting parameter. Figure 3a shows a prototypical example of this line shape. Similar to the line shape for pure background tunneling, $\mathscr{P}_{\text{interference}}$ is singular at $g = 0$ and monotonically

decays as g increases. However, $\mathscr{P}_{\text{interference}}$ is not $1/g$ (like background tunneling); therefore, the histogram's line shape should provide evidence of destructive interference features. Figure 3b confirms this idea by comparing the interference (dashed line) and background (dotted line) line shapes. Note that the histogram counts are displayed on an arbitrary log scale to highlight differences in the tails of these line shapes.

As in the case of nonresonant tunneling, eq 4 can be used to determine the histogram line shape for a system that has both an interference feature and background tunneling

$$\mathscr{P}_{\text{interference*background}}(g) \propto \int_0^g dg' \mathscr{P}_{\text{interference}}(g - g')\mathscr{P}_{\text{background}}(g') \propto \int_{g_-}^g dg' \frac{\mathscr{P}_{\text{interference}}(g - g')}{g'} \tag{12}$$

Figure 3a displays examples of this form for constant c_ω and several g_-. Not surprisingly, the combination of interference and background tunneling leads to line shapes qualitatively different than those for exclusively interference or background tunneling. For example, eq 12 shows a peak. Although the peak is very positively skewed (in qualitative agreement with some experimental results[67]), it decays asymptotically as $1/g$, which might make it blend in with the $1/g$ background.

Consequently, it is our proposal that the presence (absence) of destructive interference features in single-molecule electron transport should be reflected in the line shape of the conductance histogram. Even though our predicted peak may be largely overshadowed by the background, the line shape should still differ from $1/g$.

Finally, we examine the efficacy of quantitatively estimating c_ω from histograms. As in the case of nonresonant tunneling, we simulate and fit (to eq 12) histograms with a known value of c_ω and various amounts of background tunneling. The interference and background model has trouble fitting data in the absence of background tunneling (Figure 3b) due to the same numerical issues as $g_- \to 0$; however, the more applicable interference-only model, eq 11, estimates c_ω with ~1% error. When background tunneling is present, the interference and background model favorably estimates c_ω (≲2% error), whereas the interference-only model is quite inaccurate. As expected, the $1/g$ line shape for pure background tunneling does not describe any of the histograms well.

CONCLUSIONS

In this work, we developed models for extracting quantitative physical information from experimental break junction conductance histograms, which has historically often been limited to the most probable conductance. We instead considered the line shape of a histogram peak, showing that molecular properties directly determine the shape of the peak and that these properties can be faithfully quantified from experimental data. For the common case of transport *via* nonresonant tunneling, the line shape encodes the average level alignment and the average channel−electrode coupling of the predominant molecular channel. When a molecule with a destructive interference feature is examined, the histogram line shape should indicate an interference feature and also quantitatively reflect the steepness of the well in the transmission function.

The key to quantitatively interpreting conductance histograms for single-molecule electron transport is the inclusion of electrode−electrode tunneling. Because most molecules of interest are at most 1−2 nm long, the gap between the electrodes is sufficiently small that electrons can directly tunnel from one electrode to the other. Measured data, therefore, never contain only the molecular conductance, but a combination of molecular and such background contributions. By interpreting conductance histograms as probability density functions for the conductance observable, probability theory can be used to deconvolve these two effects.

For the purpose of quantitatively interpreting conductance histograms, our simulations showed that background tunneling *cannot* be neglected. Even though models that do not account for the background may produce reasonable qualitative fits of a histogram, they poorly estimate the underlying physical information that determines the line shape. Our simulated data, using a rectangular barrier model for the background, suggest that neglecting the background may lead to relative errors of ~25%. Finally, by considering the role of background tunneling directly in the conductance histogram, our models eliminate the perceived need for data selection. Conductance traces that do not have identifiable molecular plateaux are either captured by the $1/G$ background tunneling term or incorporated into the molecular statistics. In the end, we hope this work will provide additional tools to aid experimental characterizations of single-molecule electron transport.

METHODS

Histograms were simulated or fitted with MolStat 1.3,[68] which uses the GNU Scientific Library.[69]

Conflict of Interest: The authors declare no competing financial interest.

Acknowledgment. We thank Latha Venkataraman and her group for sharing the experimental data in Figure 1 with us. M.A.R. and M.G.R. (while at Northwestern) were supported by the U. S. Air Force Office of Scientific Research Multidisciplinary University Research Initiative (FA9550-14-1-003). M.G.R. (at Stony Brook) was supported by the Institute for Advanced Computational Science. The figures were prepared with the SciDraw package.[70]

Supporting Information Available: Derivations of eqs 5, 6, 10, and 11 and the MolStat[68] input files used to generate the histograms analyzed in Figures 2 and 3. The Supporting

Information is available free of charge on the ACS Publications website at DOI: 10.1021/acsnano.5b03183.

REFERENCES AND NOTES

1. Nitzan, A. Electron Transmission through Molecules and Molecular Interfaces. *Annu. Rev. Phys. Chem.* **2001**, *52*, 681–750.
2. McCreery, R. L. Molecular Electronic Junctions. *Chem. Mater.* **2004**, *16*, 4477–4496.
3. Cuevas, J. C.; Scheer, E. *Molecular Electronics*; World Scientific: Hackensack, NJ, 2010.
4. McCreery, R. L.; Yan, H.; Bergren, A. J. A Critical Perspective on Molecular Electronic Junctions: There Is Plenty of Room in the Middle. *Phys. Chem. Chem. Phys.* **2013**, *15*, 1065–1081.
5. Aviram, A.; Ratner, M. A. Molecular Rectifiers. *Chem. Phys. Lett.* **1974**, *29*, 277–283.
6. Paulsson, M.; Brandbyge, M. Transmission Eigenchannels from Nonequilibrium Green's Functions. *Phys. Rev. B: Condens. Matter Mater. Phys.* **2007**, *76*, 115117.
7. Büttiker, M.; Imry, Y.; Landauer, R.; Pinhas, S. Generalized Many-Channel Conductance Formula with Application to Small Rings. *Phys. Rev. B: Condens. Matter Mater. Phys.* **1985**, *31*, 6207–6215.
8. Imry, Y.; Landauer, R. Conductance Viewed as Transmission. *Rev. Mod. Phys.* **1999**, *71*, S306–S312.
9. Reed, M. A.; Zhou, C.; Muller, C. J.; Burgin, T. P.; Tour, J. M. Conductance of a Molecular Junction. *Science* **1997**, *278*, 252–254.
10. Xu, B.; Tao, N. J. Measurement of Single-Molecule Resistance by Repeated Formation of Molecular Junctions. *Science* **2003**, *301*, 1221–1223.
11. Muller, C. J.; van Ruitenbeek, J. M.; de Jongh, L. J. Experimental Observation of the Transition From Weak Link to Tunnel Junction. *Phys. C* **1992**, *191*, 485–504.
12. Muller, C. J.; van Ruitenbeek, J. M.; de Jongh, L. J. Conductance and Supercurrent Discontinuities in Atomic-Scale Metallic Constrictions of Variable Width. *Phys. Rev. Lett.* **1992**, *69*, 140–143.
13. Krans, J. M.; van Ruitenbeek, J. M.; Fisun, V. V.; Yanson, I. K.; de Jongh, L. J. The Signature of Conductance Quantization in Metallic Point Contacts. *Nature* **1995**, *375*, 767–769.
14. Reichert, J.; Ochs, R.; Beckmann, D.; Weber, H. B.; Mayor, M.; Löhneysen, H. v. Driving Current through Single Organic Molecules. *Phys. Rev. Lett.* **2002**, *88*, 176804.
15. Xiao, X.; Xu, B.; Tao, N. J. Measurement of Single Molecule Conductance: Benzenedithiol and Benzenedimethanethiol. *Nano Lett.* **2004**, *4*, 267–271.
16. Schwarz, F.; Lörtscher, E. Break-Junctions for Investigating Transport at the Molecular Scale. *J. Phys.: Condens. Matter* **2014**, *26*, 474201.
17. Xiang, D.; Jeong, H.; Lee, T.; Mayer, D. Mechanically Controllable Break Junctions for Molecular Electronics. *Adv. Mater.* **2013**, *25*, 4845–4867.
18. He, J.; Sankey, O.; Lee, M.; Tao, N.; Li, X.; Lindsay, S. Measuring Single Molecule Conductance with Break Junctions. *Faraday Discuss.* **2006**, *131*, 145–154.
19. Mayor, M.; Weber, H. B. Statistical Analysis of Single-Molecule Junctions. *Angew. Chem., Int. Ed.* **2004**, *43*, 2882–2884.
20. Venkataraman, L.; Klare, J. E.; Nuckolls, C.; Hybertsen, M. S.; Steigerwald, M. L. Dependence of Single-Molecule Junction Conductance on Molecular Conformation. *Nature* **2006**, *442*, 904–907.
21. Lörtscher, E.; Weber, H. B.; Riel, H. Statistical Approach to Investigating Transport through Single Molecules. *Phys. Rev. Lett.* **2007**, *98*, 176807.
22. Dreher, M.; Pauly, F.; Heurich, J.; Cuevas, J. C.; Scheer, E.; Nielaba, P. Structure and Conductance Histogram of Atomic-Sized Au Contacts. *Phys. Rev. B: Condens. Matter Mater. Phys.* **2005**, *72*, 075435.
23. Quek, S. Y.; Venkataraman, L.; Choi, H. J.; Louie, S. G.; Hybertsen, M. S.; Neaton, J. B. Amine–Gold Linked Single-Molecule Circuits: Experiment and Theory. *Nano Lett.* **2007**, *7*, 3477–3482.
24. Andrews, D. Q.; Van Duyne, R. P.; Ratner, M. A. Stochastic Modulation in Molecular Electronic Transport Junctions: Molecular Dynamics Coupled with Charge Transport Calculations. *Nano Lett.* **2008**, *8*, 1120–1126.
25. Paulsson, M.; Krag, C.; Frederiksen, T.; Brandbyge, M. Conductance of Alkanedithiol Single-Molecule Junctions: A Molecular Dynamics Study. *Nano Lett.* **2009**, *9*, 117–121.
26. Venkataraman, L.; Klare, J. E.; Tam, I. W.; Nuckolls, C.; Hybertsen, M. S.; Steigerwald, M. L. Single-Molecule Circuits with Well-Defined Molecular Conductance. *Nano Lett.* **2006**, *6*, 458–462.
27. Natelson, D. Mechanical Break Junctions: Enormous Information in a Nanoscale Package. *ACS Nano* **2012**, *6*, 2871–2876.
28. Engelkes, V. B.; Beebe, J. M.; Frisbie, C. D. Analysis of the Causes of Variance in Resistance Measurements on Metal–Molecule–Metal Junctions Formed by Conducting-Probe Atomic Force Microscopy. *J. Phys. Chem. B* **2005**, *109*, 16801–16810.
29. Ulrich, J.; Esrail, D.; Pontius, W.; Venkataraman, L.; Millar, D.; Doerrer, L. H. Variability of Conductance in Molecular Junctions. *J. Phys. Chem. B* **2006**, *110*, 2462–2466.
30. Fatemi, V.; Kamenetska, M.; Neaton, J. B.; Venkataraman, L. Environmental Control of Single-Molecule Junction Transport. *Nano Lett.* **2011**, *11*, 1988–1992.
31. French, W. R.; Iacovella, C. R.; Cummings, P. T. Large-Scale Atomistic Simulations of Environmental Effects on the Formation and Properties of Molecular Junctions. *ACS Nano* **2012**, *6*, 2779–2789.
32. French, W. R.; Iacovella, C. R.; Rungger, I.; Souza, A. M.; Sanvito, S.; Cummings, P. T. Structural Origins of Conductance Fluctuations in Gold-Thiolate Molecular Transport Junctions. *J. Phys. Chem. Lett.* **2013**, *4*, 887–891.
33. Gotsmann, B.; Riel, H.; Lörtscher, E. Direct Electrode-Electrode Tunneling in Break-Junction Measurements of Molecular Conductance. *Phys. Rev. B: Condens. Matter Mater. Phys.* **2011**, *84*, 205408.
34. Bâldea, I. Interpretation of Stochastic Events in Single-Molecule Measurements of Conductance and Transition Voltage Spectroscopy. *J. Am. Chem. Soc.* **2012**, *134*, 7958–7962.
35. Reuter, M. G.; Hersam, M. C.; Seideman, T.; Ratner, M. A. Signatures of Cooperative Effects and Transport Mechanisms in Conductance Histograms. *Nano Lett.* **2012**, *12*, 2243–2248.
36. Williams, P. D.; Reuter, M. G. Level Alignments and Coupling Strengths in Conductance Histograms: The Information Content of a Single Channel Peak. *J. Phys. Chem. C* **2013**, *117*, 5937–5942.
37. Zhang, G.; Ratner, M. A.; Reuter, M. G. Is Molecular Rectification Caused by Asymmetric Electrode Couplings or by a Molecular Bias Drop? *J. Phys. Chem. C* **2015**, *119*, 6254–6260.
38. Grüter, L.; González, M. T.; Huber, R.; Calame, M.; Schönenberger, C. Electrical Conductance of Atomic Contacts in Liquid Environments. *Small* **2005**, *1*, 1067–1070.
39. Jang, S.-Y.; Reddy, P.; Majumdar, A.; Segalman, R. A. Interpretation of Stochastic Events in Single Molecule Conductance Measurements. *Nano Lett.* **2006**, *6*, 2362–2367.
40. Vilan, A. Analyzing Molecular Current-Voltage Characteristics with the Simmons Tunneling Model: Scaling and Linearization. *J. Phys. Chem. C* **2007**, *111*, 4431–4444.
41. Haiss, W.; van Zalinge, H.; Higgins, S. J.; Bethell, D.; Höbenreich, H.; Schiffrin, D. J.; Nichols, R. J. Redox State Dependence of Single Molecule Conductivity. *J. Am. Chem. Soc.* **2003**, *125*, 15294–15295.
42. Haiss, W.; Nichols, R. J.; van Zalinge, H.; Higgins, S. J.; Bethell, D.; Schiffrin, D. J. Measurement of Single Molecule Conductivity using the Spontaneous Formation of Molecular Wires. *Phys. Chem. Chem. Phys.* **2004**, *6*, 4330–4337.
43. González, M. T.; Wu, S.; Huber, R.; van der Molen, S. J.; Schönenberger, C.; Calame, M. Electrical Conductance of

Molecular Junctions by a Robust Statistical Analysis. *Nano Lett.* **2006**, *6*, 2238–2242.
44. Li, X.; He, J.; Hihath, J.; Xu, B.; Lindsay, S. M.; Tao, N. Conductance of Single Alkanedithiols: Conduction Mechanism and Effect of Molecule−Electrode Contacts. *J. Am. Chem. Soc.* **2006**, *128*, 2135–2141.
45. Ghahramani, S. *Fundamentals of Probability*, 2nd ed.; Prentice-Hall: Upper Saddle River, NJ, 2000.
46. Sautet, P.; Joachim, C. Electronic Interference Produced by a Benzene Embedded in a Polyacetylene Chain. *Chem. Phys. Lett.* **1988**, *153*, 511–516.
47. Baer, R.; Neuhauser, D. Phase Coherent Electronics: A Molecular Switch Based on Quantum Interference. *J. Am. Chem. Soc.* **2002**, *124*, 4200–4201.
48. Ernzerhof, M.; Zhuang, M.; Rocheleau, P. Side-Chain Effects in Molecular Electronic Devices. *J. Chem. Phys.* **2005**, *123*, 134704.
49. Cardamone, D. M.; Stafford, C. A.; Mazumdar, S. Controlling Quantum Transport through a Single Molecule. *Nano Lett.* **2006**, *6*, 2422–2426.
50. Solomon, G. C.; Andrews, D. Q.; Hansen, T.; Goldsmith, R. H.; Wasielewski, M. R.; Van Duyne, R. P.; Ratner, M. A. Understanding Quantum Interference in Coherent Molecular Conduction. *J. Chem. Phys.* **2008**, *129*, 054701.
51. Solomon, G. C.; Andrews, D. Q.; Goldsmith, R. H.; Hansen, T.; Wasielewski, M. R.; Van Duyne, R. P.; Ratner, M. A. Quantum Interference in Acyclic Systems: Conductance of Cross-Conjugated Molecules. *J. Am. Chem. Soc.* **2008**, *130*, 17301–17308.
52. Yoshizawa, K.; Tada, T.; Staykov, A. Orbital Views of the Electron Transport in Molecular Devices. *J. Am. Chem. Soc.* **2008**, *130*, 9406–9413.
53. Solomon, G. C.; Andrews, D. Q.; Van Duyne, R. P.; Ratner, M. A. Electron Transport through Conjugated Molecules: When the π System Only Tells Part of the Story. *ChemPhysChem* **2009**, *10*, 257–264.
54. Markussen, T.; Stadler, R.; Thygesen, K. S. The Relation between Structure and Quantum Interference in Single Molecule Junctions. *Nano Lett.* **2010**, *10*, 4260–4265.
55. Reuter, M. G.; Hansen, T. Finding Destructive Interference Features in Molecular Transport Junctions. *J. Chem. Phys.* **2014**, *141*, 181103.
56. Bergfield, J. P.; Barr, J. D.; Stafford, C. A. The Number of Transmission Channels Through a Single-Molecule Junction. *ACS Nano* **2011**, *5*, 2707–2714.
57. Frisenda, R.; Perrin, M. L.; Valkenier, H.; Hummelen, J. C.; van der Zant, H. S. J. Statistical Analysis of Single-Molecule Breaking Traces. *Phys. Status Solidi B* **2013**, *250*, 2431–2436.
58. Kim, T.; Darancet, P.; Widawsky, J. R.; Kotiuga, M.; Quek, S. Y.; Neaton, J. B.; Venkataraman, L. Determination of Energy Level Alignment and Coupling Strength in 4,4′-Bipyridine Single-Molecule Junctions. *Nano Lett.* **2014**, *14*, 794–798.
59. Cohen-Tannoudji, C.; Diu, B.; Laloë, F. *Quantum Mechanics*; John Wiley & Sons: New York, 1977.
60. Fracasso, D.; Valkenier, H.; Hummelen, J. C.; Solomon, G. C.; Chiechi, R. C. Evidence for Quantum Interference in SAMs of Arylethynylene Thiolates in Tunneling Junctions with Eutectic Ga-In (EGaIn) Top-Contacts. *J. Am. Chem. Soc.* **2011**, *133*, 9556–9563.
61. Hong, W.; Valkenier, H.; Mészáros, G.; Manrique, D. Z.; Mishchenko, A.; Putz, A.; García, P. M.; Lambert, C. J.; Hummelen, J. C.; Wandlowski, T. An MCBJ Case Study: The Influence of π-Conjugation on the Single-Molecule Conductance at a Solid/Liquid Interface. *Beilstein J. Nanotechnol.* **2011**, *2*, 699–713.
62. Taniguchi, M.; Tsutsui, M.; Mogi, R.; Sugawara, T.; Tsuji, Y.; Yoshizawa, K.; Kawai, T. Dependence of Single-Molecule Conductance on Molecule Junction Symmetry. *J. Am. Chem. Soc.* **2011**, *133*, 11426–11429.
63. Aradhya, S. V.; Meisner, J. S.; Krikorian, M.; Ahn, S.; Parameswaran, R.; Steigerwald, M. L.; Nuckolls, C.; Venkataraman, L. Dissecting Contact Mechanics from Quantum Interference in Single-Molecule Junctions of Stilbene Derivatives. *Nano Lett.* **2012**, *12*, 1643–1647.
64. Guédon, C. M.; Valkenier, H.; Markussen, T.; Thygesen, K. S.; Hummelen, J. C.; van der Molen, S. J. Observation of Quantum Interference in Molecular Charge Transport. *Nat. Nanotechnol.* **2012**, *7*, 305–309.
65. Kaliginedi, V.; Moreno-García, P.; Valkenier, H.; Hong, W.; García-Suárez, V. M.; Buiter, P.; Otten, J. L. H.; Hummelen, J. C.; Lambert, C. J.; Wandlowski, T. Correlations between Molecular Structure and Single-Junction Conductance: A Case Study with Oligo(phenylene-ethynylene)-Type Wires. *J. Am. Chem. Soc.* **2012**, *134*, 5262–5275.
66. Arroyo, C. R.; Tarkuc, S.; Frisenda, R.; Seldenthuis, J. S.; Woerde, C. H. M.; Eelkema, R.; Grozema, F. C.; van der Zant, H. S. J. Signatures of Quantum Interference Effects on Charge Transport Through a Single Benzene Ring. *Angew. Chem., Int. Ed.* **2013**, *52*, 3152–3155.
67. Valkenier, H.; Guédon, C. M.; Markussen, T.; Thygesen, K. S.; van der Molen, S. J.; Hummelen, J. C. Cross-Conjugation and Quantum Interference: a General Correlation? *Phys. Chem. Chem. Phys.* **2014** *16*, 653–662.
68. *MolStat*, https://bitbucket.org/mgreuter/molstat (accessed May 26, 2015).
69. Galassi, M.; Davies, J.; Theiler, J.; Gough, B.; Jungman, G.; Alken, P.; Booth, M.; Rossi, F. *GNU Scientific Library Reference Manual*, 3rd ed.; Network Theory Ltd.: U.K., 2009.
70. Caprio, M. A. LevelScheme: A Level Scheme Drawing and Scientific Figure Preparation System for Mathematica. *Comput. Phys. Commun.* **2005**, *171*, 107–118.